

Localization of a Bose Einstein condensate in an optical superlattice

Aranya B Bhattacherjee

Department of Physics, Atma Ram Sanatan Dharma College (University of Delhi, South Campus), Daula Kuan, New Delhi-110021, India

Abstract: The Bloch and dipole oscillations of a Bose Einstein condensate (BEC) in an optical superlattice is investigated. We show that the effective mass increases in an optical superlattice, which leads to localization of the BEC, in accordance with recent experimental observations [16]. In addition, we find that the secondary optical lattice is a useful additional tool to manipulate localized excitations.

1. Introduction

Interference pattern of intersecting laser beams create a periodic potential for atoms, which is known as an optical lattice [1]. Ultracold bosons trapped in such periodic potentials have been widely used recently as a model system for the study of some fundamental concepts of quantum physics. Josephson effects [2], squeezed states [3], Landau-Zener tunneling and Bloch oscillations [4] and superfluid-Mott insulator transition [5] are some examples. An important promising application under study is quantum computation in optical lattices [6]. Optical lattices are therefore, of particular interest from the perspective of both fundamental quantum physics and its connection to applications.

Using superposition of optical lattices with different periods [7], it is now possible to generate periodic potentials characterized by a richer spatial modulation, the so-called optical superlattices. The light-shifted potential of the superlattice is described as

$$V(z) = V_1 \cos^2 \left(\frac{\pi z}{d_1} \right) + V_2 \cos^2 \left(\frac{\pi z}{d_2} + \varphi \right) \quad (1)$$

Here d_1 and $d_2 > d_1$ are respectively, the primary and secondary lattice constants. V_1 and V_2 are the respective amplitudes. The secondary lattice acts as a perturbation and hence $V_2 < V_1$. φ is the phase of the secondary lattice. Theoretical interest in optical superlattice started only recently. These include work on fractional filling Mott insulator domains [8], dark [9] and gap [10] solitons, the Mott-Peierls transition [11], non-mean field effects [12] an phase diagram of BEC in two color superlattices [13]. In a recent work, the analogue of the optical branch in solid-state physics was predicted in an optical superlattice [14]. A detailed theoretical study of the Bloch and Bogoliubov spectrum of a BEC in a one-dimensional optical superlattice has been done [15]. In a very recent interesting experiment [16], it was observed that the center of mass motion of a BEC is blocked in a quasi-periodic lattice. Considering the fact that these optical superlattices are now being realized experimentally and interesting experiments are being done routinely, we were motivated to study the influence of the secondary lattice on Bloch oscillations and dipole oscillations of atoms.

2. Bloch Oscillations

We consider an elongated cigar shaped BEC confined in a harmonic trap potential $V_{ho}(r, z) = \frac{M}{2} (\omega_r^2 r^2 + \omega_z^2 z^2)$ and a one-dimensional tilted optical superlattice of the form $V_{op}(z) = E_R \left(s_1 \cos^2 \left(\frac{\pi z}{d} \right) + s_2 \cos^2 \left(\frac{\pi z}{2d} \right) \right) + mgz$. We have taken a particular case of $d_2 = 2d_1 = 2d$. s_1 and s_2 are the dimensionless amplitudes of the primary and the secondary superlattice potentials with $s_1 > s_2$. $E_R = \hbar^2 \pi^2 / 2Md^2$ is the recoil energy

$(\omega_R = \frac{E_R}{\hbar}$ is the corresponding recoil frequency) of the primary lattice. We take $\omega_r \gg \omega_z$ so that an elongate cigar shaped BEC is formed. The harmonic oscillator frequency corresponding to small motion about the minima of the optical superlattice is $\omega_s \approx \sqrt{s_1 \hbar \pi^2} \frac{1}{Md^2}$. The peak densities in each well match a Gaussian profile. Since the array is tilted, the atoms undergo coherent Bloch oscillations driven by the interwell gravitational potential mgz . The BEC is initially loaded into the primary lattice and the secondary lattice is switched on slowly. The frequency of each minima of the primary lattice is not perturbed significantly by the addition of the secondary lattice. $\omega_s \gg \omega_z$ so that the optical lattice dominates over the harmonic potential along the z-direction and hence the harmonic potential is neglected. The strong laser intensity will give rise to an array of several quasi-two-dimensional pancake shaped condensates. Because of the quantum tunneling, the overlap between the wave functions between two consecutive layers can be sufficient to ensure full coherence. We now study the Bloch dynamics of the BEC in the tilted optical superlattice by solving the discrete nonlinear schroedinger equation (DNLSE). The dynamics of the BEC is governed by the Gross-Pitaevskii equation (GPE)

$$i\hbar \frac{\partial \zeta}{\partial t} = -\frac{\hbar^2}{2m} \nabla^2 \zeta + \left\{ V_{ho}(r, z) + V_{op}(z) + g_o |\zeta|^2 \right\} \zeta \quad (2)$$

where $g_o = \frac{4\pi\hbar^2 a}{m}$, with a the two body scattering length and m the atomic mass. In the tight binding approximation the condensate order parameter can be written as

$$\zeta(r, t) = \sqrt{N_T} \sum_j \psi_j(t) \phi(r - r_j) \quad (3)$$

where N_T is the total number of atoms and $\phi(r - r_j)$ is the condensate wavefunction localized in the trap j with $\int dr \phi_j \phi_{j+1} \approx 0$, and $\int dr |\phi_j|^2 = 1$. $\psi_j(t)$ is the j^{th} amplitude. $\psi_j(t) = \sqrt{\rho_j(t)} \exp(i\theta_j(t))$, $\rho_j = \frac{N_j}{N_T}$, where N_j and θ_j are the number of particles and phases in the trap j . Substituting the ansatz (3) in (2), we find that the GPE reduces to the DNLSE.

$$i \frac{\partial \psi_j}{\partial t} = -\frac{1}{2} \left\{ (1 - \alpha(-1)^{j-1}) \psi_{j-1} + (1 - \alpha(-1)^j) \psi_{j+1} \right\} + \left(\epsilon_j + \Lambda |\psi_j|^2 \right) \psi_j \quad (4)$$

where $\varepsilon_j = \frac{1}{J_0} \int dr \left[\frac{\hbar^2}{2m} (\bar{\nabla} \phi_j)^2 + (V_{ho}(r) + V_{op}(z)) |\phi_j|^2 \right]$, $\Lambda = \frac{g_0 N}{J_0} \int dr |\phi_j|^4$, $\alpha = \Delta_0 / 2J_0$.

One can show using $J_j = - \int dr \left[\frac{\hbar^2}{2m} \bar{\nabla} \phi_j \bullet \bar{\nabla} \phi_{j+1} + \phi_j (V_{ho}(r) + V_{op}(r)) \phi_{j+1} \right]$ that there are distinctly, two Josephson coupling parameters $J_0 \pm \Delta_0 / 2$ [15]. We have rescaled time as $t \rightarrow \hbar / 2J_0 t$. In eqn(4), $\varepsilon_j = \omega_B j$. $\omega_B = mg\lambda_1 / 4J_0$ is the frequency of Bloch oscillation and λ_1 is the wavelength of the laser creating the primary lattice.

Let us now first analyze the DNLSE (eqn.4). We write ψ_j as

$$\psi_j(t) = g_j(t) \exp(i2kd - i\omega_B t) j \quad (5)$$

Note that now the periodicity of the system is that of the secondary lattice i.e. $2d$. The amplitudes g_j are site dependent and there are two distinct amplitudes [15]. k is the quasimomentum. Using equation (4), equation (5) can be written in the form,

$$\begin{aligned} i\dot{g}_j &= -\frac{1}{2} \left[(1 - (-1)^j \alpha) g_{j+1} \exp(i2kd - i\omega_B t) + (1 - (-1)^{j-1} \alpha) g_{j-1} \exp(-i2kd + i\omega_B t) \right] \\ &+ \Lambda |g_j|^2 g_j \end{aligned} \quad (6)$$

We are interested in solution of equation (6) for $k = 0$, which is the ground state of the system. We look for solutions of equation (6) as $g_j(t) = g_j(0) \exp(i \int \lambda(t) dt)$. $\lambda(t)$ is the lowest eigenvalues which is found to be,

$$\lambda(t) = \sqrt{\cos^2(\omega_B t) + \alpha^2 \sin^2(\omega_B t)} - \Lambda n_0 \quad (7)$$

In deriving equation (7), we have assumed the periodic boundary condition $g_{j+1} = g_{j-1}$. Finally the amplitudes $g_j(t)$ are

$$g_j(t) = g_j(0) \exp \left(i \frac{E[t, m]}{\omega_B} - i \Lambda n_0 t \right) \quad (8)$$

where $E[t, m]$ is the Elliptic integral of the first kind and $m = 4J_0^2 - \Delta_0^2 / 4J_0^2 = 1 - \alpha^2$.

Equation (8) represents the well-known Bloch oscillations.

Figure 1 shows a plot of $E^*(t) = \frac{E[t, m]}{\omega_B} - \Lambda n_0 t$ for $\alpha^2 = 0.6$ (solid line) and 0.2 (dashed line), $\omega_B = 2$, $\Lambda n_0 = 0.1$. It is evident from figure 1 that the effect of the secondary lattice (i.e. a finite Δ_0) is to suppress the Bloch oscillations. A similar damping of the dipole oscillation due to the secondary lattice was reported in [16]. The above simple analysis is not able to reveal the physics behind such damping. In order to understand the mechanism better, we solve the DNLSE using a variational approach adopted from [17]. The Hamiltonian function corresponding to the DNLSE (equation 4) reads

$$H = \sum_j \left[-\frac{1}{4} \left\{ (1 - (-1)^j \alpha) (\psi_j \psi_{j+1}^* + \psi_j^* \psi_{j+1}) + (1 - (-1)^{j-1} \alpha) (\psi_j \psi_{j-1}^* + \psi_j^* \psi_{j-1}) \right\} + \epsilon_j |\psi_j|^2 + \frac{\Lambda}{2} |\psi_j|^4 \right] \quad (9)$$

Where $\sum_j |\psi_j|^2 = 1$. To analyze the Bloch dynamics, we study the dynamical evolution of a site dependent Gaussian wavepacket, which we parametrize as

$$\psi_j(t) = \sqrt{K} \exp \left[-\frac{(j - \xi)^2}{\gamma^2} + ip(j - \xi) + i \frac{\delta}{2} (j - \xi)^2 + i(-1)^j \frac{\varphi}{2} \right] \quad (10)$$

Where $\xi(t)$ and $\gamma(t)$ are, respectively, the center and width of the condensate, $p(t)$ and $\delta(t)$ their associated momenta, and $K(\gamma, \xi)$ a normalization factor. $(-1)^j \frac{\varphi}{2}$ is the phase of the wave packet at the j^{th} site. Clearly depending upon whether j is odd or even, the phase is $\pm \frac{\varphi}{2}$.

The dynamics of the wave packet can be obtained by a variational principle from the Lagrangian $L = \sum_j i \psi_j \psi_j^* - H$, with the equations of motion for the variational parameters $q_i(t) = \xi, \gamma, p, \delta, \varphi$ given by $\frac{d}{dt} \frac{\partial L}{\partial \dot{q}_i} = \frac{\partial L}{\partial q_i}$. The Lagrangian is derived as

$$L = p \dot{\xi} - \frac{\gamma^2 \delta}{8} - \left[\frac{\Lambda}{2\sqrt{\pi}\gamma} \right] + \{\cos \varphi \cos p + \alpha \sin \varphi \sin p\} \exp(-\eta) - V(\gamma, \xi) \quad (11)$$

where $\eta = \frac{1}{2\gamma^2} + \frac{\gamma^2 \delta^2}{8}$ and $V(\gamma, \xi) = K \int_{-\infty}^{\infty} dj \epsilon_j \exp \left(-2 \frac{(j - \xi)^2}{\gamma^2} \right)$.

The variational equations of motion are derived as

$$\dot{p} = -\frac{\partial V}{\partial \xi} \quad (12a)$$

$$\dot{\xi} = [\cos \varphi \sin p - \alpha \sin \varphi \cos p] \exp(-\eta) \quad (12b)$$

$$\dot{\delta} = [\cos \varphi \cos p + \alpha \sin \varphi \sin p] \exp(-\eta) \left[\frac{4}{\gamma^4} - \delta^2 \right] + \frac{2\Lambda}{\gamma^3 \sqrt{\pi}} - \frac{4}{\gamma} \frac{\partial V}{\partial \gamma} \quad (12c)$$

$$\dot{\gamma} = \gamma \delta [\cos \varphi \cos p + \sin \varphi \sin p] \exp(-\eta) \quad (12d)$$

$$\tan \varphi = \alpha \tan p \quad (12e)$$

Since $\cos^2 \varphi + \sin^2 \varphi = 1$, together with equation (12e), we get the constraints on $\cos \varphi$ and $\sin \varphi$,

$$\begin{aligned} \cos \varphi &= \frac{\cos p}{\sqrt{\cos^2 p + \alpha^2 \sin^2 p}}, \\ \sin \varphi &= \frac{\alpha \sin p}{\sqrt{\cos^2 p + \alpha^2 \sin^2 p}} \end{aligned} \quad (13)$$

Corresponding to the variational equations (12) and (13), the effective Hamiltonian is written as

$$H = \frac{\Lambda}{2\sqrt{\pi}\gamma} - \cos p \sqrt{1 + \alpha^2 \tan^2 p} \exp(-\eta) + V(\gamma, \xi) \quad (14)$$

In the following we study the Bloch and dipole oscillations. We first consider a tilted periodic potential as before. The on site energies for this case is written as $\varepsilon_j = j\omega_B$.

Using equations (12), we find $V = \xi \omega_B$ and $\dot{p} = -\omega_B$.

We solve the variational equations of motion numerically for the following initial values $\xi(0) = 0$, $p(0) = 0$, $\delta(0) = 0$, $\gamma(0) = 10$ and the parameters $\Lambda = 10$, $\omega_B = 2$. The result for the center of mass $\xi(t)$ is depicted in figure 2 for two different values of $\alpha = 0.1$ (dashed line) and $\alpha = 0.6$ (bold line). Clearly on increasing the strength of the secondary lattice, the amplitude of the center of mass motion reduces. Optical superlattices with higher periodicities will block the center of mass more strongly. This perhaps is analogous to the Anderson localization of a particle placed in a lattice with disordered on-site energies

[18]. In order to understand the origin of this blocking of center of mass motion, we derive the effective mass $(m^*)^{-1} = \partial^2 H / \partial p^2$ as,

$$m^* = \frac{(1 + \alpha^2 \tan^2 p)^{3/2} \exp(\eta)}{\cos p (1 - \alpha^2 \tan^4 p) (1 - \alpha^2)} \quad (15)$$

A diverging effective mass $m^* \rightarrow \infty$ as $t \rightarrow \infty$ due to interactions leads to a self-trapping of the wave packet [17].

It is interesting to note that, we now have an additional handle α to tune the effective mass. A plot between m^* and α in fig.3 shows that as the strength of the secondary lattice increases, the effective mass also increases. Therefore the origin of the Anderson type localization in an optical superlattice is due to an increase in the effective mass.

3. Dipole Oscillations

We now study the dipole oscillations. Instead of the gravitational potential, we now consider a sufficiently large ($\omega_z > \omega_s$) magnetic harmonic potential superimposed on the optical lattice $\varepsilon_j = \Omega j^2$, with $\Omega = m\omega_z^2\lambda_1^2/8$. λ_1 is the wave length of the primary lattice.

The variational equations of motion now give $V(\gamma, \xi) = \Omega \left(\frac{\gamma^2}{4} + \xi^2 \right)$ and $\dot{p} = -2\Omega\xi$. In the regime of negligible mean field interaction ($\Lambda = 0$) and small momenta p , the equation for the center of mass is $\dot{\xi}(t) \approx \sqrt{1 - \alpha^2} p$. Consequently the center of mass obeys the equation of an undamped harmonic oscillator $\ddot{\xi} = \omega_d^2 \xi$, where the frequency of dipole oscillation $\omega_d^2 = 2\Omega\sqrt{1 - \alpha^2}$ is reduced in the presence of the secondary lattice. In actual experiments [16], to excite the dipole oscillations, the center of the magnetic trap is shifted abruptly. This corresponds to the initial conditions $\xi(0) = 0$ and $p(0) = p_0$. The

center of mass in the $\Lambda = 0$ regime and small momenta is $\xi(t) \approx \frac{(1 - \alpha^2)^{1/4} p_0}{\sqrt{2\Omega}} \sin \omega_d t$. In

the low momenta limit, the amplitude of the center of mass decreases with increasing

strength of the secondary lattice approximately as $\left[1 - \left(\frac{s_2}{s_1} \left(\frac{\pi^2}{2} - 2 \right) \right)^2 \right]^{1/4}$. At higher

momentum, dynamical instability sets in and it becomes difficult to separate and isolate the effect of secondary lattice induced localization and the dynamical instability. The initial value of the effective mass can be positive ($\cos p_0 > 0$) or negative ($\cos p_0 < 0$).

Let us suppose that $\cos p_0 > 0$ and initial values $\gamma_0, \delta_0 = 0$ and $\xi_0 = 0$. The initial

value of the Hamiltonian is $H_0 = \frac{\Lambda}{2\sqrt{\pi}\gamma_0} - \cos p_0 \sqrt{1+\alpha^2 \tan^2 p_0} \exp\left(-\frac{1}{2}\gamma_0^2\right) + \frac{\Omega\gamma_0^2}{4}$.

Since the Hamiltonian is conserved, we have

$$H_0 = \frac{\Lambda}{2\sqrt{\pi}\gamma_0} - \cos p_0 \sqrt{1+\alpha^2 \tan^2 p_0} \exp\left(-\frac{1}{2}\gamma_0^2 - \frac{\gamma^2 \delta^2}{8}\right) + \frac{\Omega\gamma_0^2}{4}. \quad \text{The parabolic}$$

external potential helps to keep $H_0 > 0$. Therefore

$$\frac{\Lambda}{2\sqrt{\pi}\gamma} + \frac{\Omega\gamma^2}{4} - H_0 > 0 \quad (16)$$

Equation (16) is cubic in γ and we see that when $H_0 > 0$, the width γ has to remain finite and that γ approaches the root γ_f of equation (16), which is nearest to γ_0 . Now the final value of γ (i.e. γ_f) can be less or greater than γ_0 depending on the trap frequency Ω and nonlinear coefficient Λ . In the experiment of ref.[16], $\omega_z \approx 2\pi \times 10$ Hz and $\lambda_l \approx 830 \times 10^{-9}$ nm. This corresponds to a very low value of Ω (dimensionless units) ≈ 0.0001 . At low values of the interaction ($\Lambda = 10$) and low Ω ($= 0.0001$), $\gamma_f > \gamma_0$ and increases with increasing Ω . On the other hand at high values of the interactions ($\Lambda = 100$), there is hardly any variation of γ_f with Ω . Fig. 4 shows a plot of the dipole oscillations for two values of the parameter $\alpha = 0.1$ (dashed line), $\alpha = 0.7$ (bold line), $\xi_0 = 0$, $p_0 = 0.1$, $\delta_0 = 0$, $\gamma_0 = 40$, $\Lambda = 5$, $\Omega = 0.0002$. We notice that increasing the strength of the secondary lattice, the dipole oscillations are blocked, in accordance with the experimental observations [16]. This reduction in the amplitude of the dipole oscillation on increasing the strength of the secondary lattice is due to an increase in the effective mass as mentioned earlier. Since in this case $\delta(t) \rightarrow \infty$ as $t \rightarrow \infty$, the motion is highly damped and the condensate is trapped. We also find that the final value of center of mass ξ_f is not the same as ξ_0 .

When $H_0 < 0$ (for very small values of Λ and Ω), the wavefunction of the condensate spreads (diffusion) since $\gamma \rightarrow \infty$ as $t \rightarrow \infty$. The transition between the trapped state and diffusive state occurs at $H_0 = 0$ i.e. when the interaction parameter Λ takes the value

$$\Lambda_c = 2\sqrt{\pi}\gamma_0 \cos p_0 \sqrt{1+\alpha^2 \tan^2 p_0} \exp\left(-\frac{1}{2}\gamma_0^2\right) - \frac{\Omega\sqrt{\pi}\gamma_0^3}{2} \quad (17)$$

On increasing the trap frequency Ω , Λ_c decreases while on the other hand on increasing the strength of the secondary lattice, Λ_c increases.

For the $H_0 > 0$ case, increasing the trap frequency $\Omega \approx 0.01$ (this corresponds to $\omega_z \approx 2\pi \times 100$ Hz), γ_f is actually smaller than γ_0 as Ω increases. This behaviour can be understood by looking at equations 12(c) and 12(d). For a certain combination of

parameters (high Ω), we can have stationary solutions i.e. $\dot{\gamma} = 0$ and $\dot{\delta} = 0$ i.e. $\delta(t) = \delta_0 = 0$ and $\gamma(t) = \gamma_0$, when the nonlinear coefficient is equal to

$$\Lambda_s = \sqrt{\pi}\Omega\gamma_0^3 - \frac{2\sqrt{\pi}\cos p_0\sqrt{1+\alpha^2\tan^2 p_0}\exp(-\frac{1}{2}\gamma_0^2)}{\gamma_0} \quad (18)$$

This implies that the wave packet moves without changing its shape. The effect of Ω and α on Λ_s is opposite to that observed for Λ_c . From equation (18), we see that if $\cos p_0 < 0$, then the value of Λ needed to have a stationary solution is higher compared to the case $\cos p_0 > 0$. Further more for $\cos p_0 < 0$, we observe that

$$H_0 = \frac{\Lambda}{2\sqrt{\pi}\gamma_0} + |\cos p_0|\sqrt{1+\alpha^2\tan^2 p_0}\exp(-\frac{1}{2}\gamma_0^2) + \frac{\Omega\gamma_0^2}{4} > 0 \quad \text{and}$$

$$\frac{\Lambda}{2\sqrt{\pi}\gamma} + \frac{\Omega\gamma^2}{4} = H_0 - |\cos p_0|\sqrt{1+\alpha^2\tan^2 p_0}\exp(-\frac{1}{2}\gamma_0^2). \quad \text{Therefore}$$

$H_0 > |\cos p_0|\sqrt{1+\alpha^2\tan^2 p_0}$, the width γ has to remain finite. For $H_0 < |\cos p_0|\sqrt{1+\alpha^2\tan^2 p_0}$, $\alpha \rightarrow \infty, \delta \rightarrow 0$. This transition occurs at

$$\Lambda_c = 2\sqrt{\pi}\gamma_0|\cos p_0|\sqrt{1+\alpha^2\tan^2 p_0}\left(1 - \exp(-\frac{1}{2}\gamma_0^2)\right) - \frac{\sqrt{\pi}\Omega\gamma_0^3}{2} \quad (19)$$

There is an intermediate regime $\Lambda_c < \Lambda < \Lambda_s$ when $\delta(t)$ and $\gamma(t)$ have oscillatory solutions. These are termed as breathers [17]. The breather regime increases with increasing trap frequency Ω . For $\cos p_0 > 0$, the breather regime decreases with increasing strength of the secondary lattice.

4. Conclusions

In conclusion, we have studied the Bloch and dipole oscillations of a Bose Einstein condensate trapped in an optical superlattice. In particular, we have shown that due to the addition of the secondary lattice, the center of mass motion is blocked which leads to an Anderson type localization of the BEC. This effect is due to an increase in the effective mass in the presence of the secondary lattice. Increasing the strength of the secondary lattice increases the effective mass and hence an increased blocking of the center of mass motion. The frequency of the dipole oscillations is also found to be reduced due to the secondary lattice. This result is in accordance with recent experiments [16]. We have also shown that localized excitations such as breathers and stationary solutions can be controlled by strength of the secondary lattice, the magnetic trap frequency and the interatomic interactions.

References

- [1] O. Morsch and M. Oberthaler, Rev. Mod. Phy., **78**, 179 (2006).
- [2] B. P. Anderson and M. A. Kasevich, Science, **282**, 1686 (1998).
- [3] C. Orzel, A. K. Tuchman, M. L. Fenselau, M. Yasuda and M. A. Kasevich, Science, **291**, 2386 (2001).
- [4] O. Morsch, J. H. Müller, M. Cristiani, D. Ciampini and E. Arimondo, Phys. Rev. Letts., **87**, 140402 (2001).
- [5] M. Greiner, O. Mandel, T. Esslinger, T. W. Hänsch, I. Bloch, Nature, **415**, 39 (2002).
- [6] J. Sebby-Strabley et. al. Phys. Rev A, **73**, 033605 (2006).
- [7] S. Peil et. al. Phys. Rev. Letts., **67**, 051603 (R) (2003).
- [8] P. Buonsante and A. Vezzani, Phys. Rev. A, **70**, 033608 (2004); P. Buonsante, V. Penna and A. Vezzani, Phys. Rev. A, **70**, 061603 (R), (2004); P. Buonsante, V. Penna and A. Vezzani, Phys. Rev. A, **72**, 013614 (2005); p. Buonsante, V. Penna and A. Vezzani, Laser Physics, **15** (2), 361 (2005).
- [9] P. J. Y. Louis, E. A. Ostrovskaya and Y. S. Kivshar, J. Opt. B, **6**, S309 (2004).
- [10] P. J. Y. Louis, E. A. Ostrovskaya and Y. S. Kivshar, Phys. Rev. A, **71**, 023612 (2005), M .A. Porter, P. G. Kevrekidis, R. Carretero-Gonzalez and D. J. Frantzeskakis, Condmat/0507676.
- [11] L. A. Dmitrieva and Y. A. Kuperin, Cond-mat/0311468.
- [12] A. M. Rey, B. L. Hu, E. Calzetta, A. Roura and C. W. Clark, Phys. Rev. A, **69**, 033610 (2004).
- [13] R. Roth and K. Burnett, Phys. Rev. A, **68**, 023604 (2003).
- [14] Chou-Chun Huang and Wen-Chin Wu, Phys. Rev. A, **72**, 065601 (2005).
- [15] A. Bhattacherjee, J. Phys.B. At. Mol. Opt. Phys. **40**, 143 (2007).
- [16] J.E. Lye et. al. Cond-Mat/0611146.
- [17] A. Trombettoni and A. Smerzi, Phys. Letts A, **86**, 2353 (2001).
- [18] P.W. Anderson, Phys. Rev. **109**, 1492 (1958).

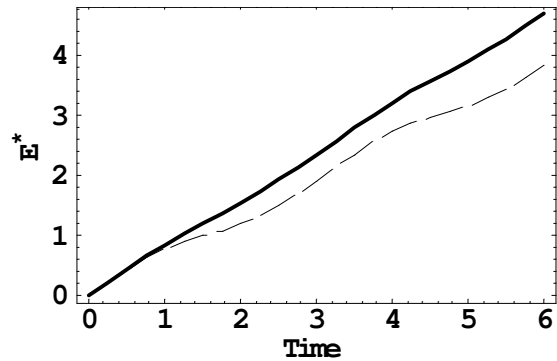


Figure 1: A plot of $E^*(t) = \frac{E[t, m]}{\omega_B} - \Lambda n_0 t$ for $\alpha^2 = 0.6$ (solid line) and 0.2 (dashed line), $\omega_B = 2$, $\Lambda n_0 = 0.1$. It is evident that as the strength of the secondary lattice increases the amplitude of the Bloch oscillation decreases.

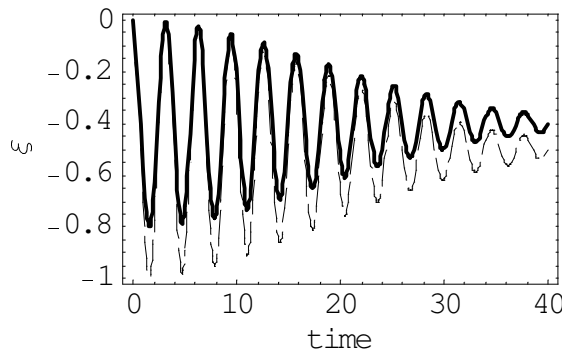


Figure 2: Oscillations of the center of mass $\xi(t)$ is depicted for two different values of $\alpha = 0.1$ (dashed line) and $\alpha = 0.6$ (bold line). Clearly on increasing the strength of the secondary lattice, the amplitude of the center of mass motion reduces.

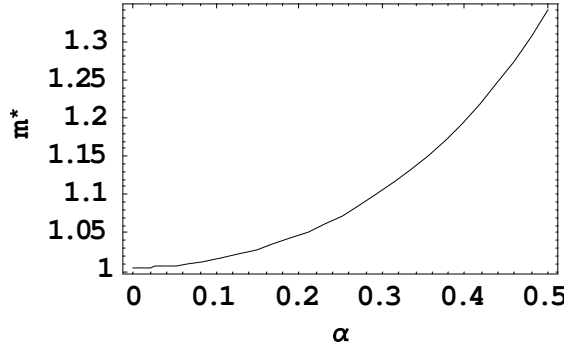


Figure 3: A plot between m^* and α shows that as the strength of the secondary lattice increases, the effective mass also increases. Therefore the origin of the Anderson type localization in an optical superlattice is due to an increase in the effective mass.

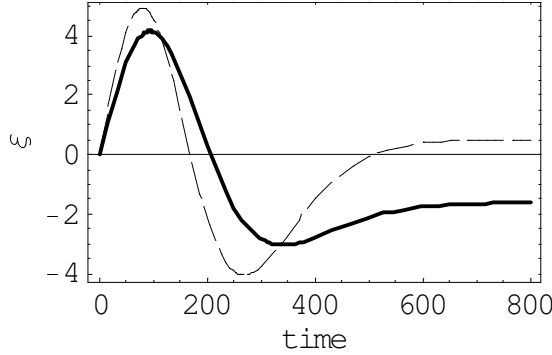


Figure 4: A plot of the dipole oscillations for two values of the parameter $\alpha = 0.1$ (dashed line), $\alpha = 0.7$ (bold line), $\xi_0 = 0$, $p_0 = 0.1$, $\delta_0 = 0$, $\gamma_0 = 40$, $\Lambda = 5$, $\Omega = 0.0002$. We notice that increasing the strength of the secondary lattice, the dipole oscillations are blocked, in accordance with the experimental observations of reference [16]. This reduction in the amplitude of the dipole oscillation on increasing the strength of the secondary lattice is due to an increase in the effective mass as mentioned earlier.